ANALYSIS OF ACCURACY AT BALLISTIC RE-ENTRY IN THE EARTH ATMOSPHERE

Yu. G. Sikharulidze*, P. Moraes Jr.**, A. N. Korchagin*

*Keldysh Institute of Applied Mathematics RAS, Russia , E-mail: sikh@iae.cta.br
**CTA/ Instituto de Aeronáutica e Espaço , Brasil, E-mail: moraes@iae.cta.br

Abstract

The problem of delivery experimental and observation results from orbit to the Earth arises very often in the process of space research. The simplest and cheapest solution of the problem is the use of a small ballistic re-entry vehicle. Such kind of vehicle has no control system for motion into the atmosphere. So, this produces significant dispersion of landing point that complicates search of the vehicle and very often a safe landing. The paper includes an analysis of the accuracy problem for ballistic re-entry in the Earth disturbed atmosphere and choice of optimal re-entry conditions. Besides the common initial re-entry conditions and ballistic coefficient of the vehicle it considers the influence of the re-entry point latitude, initial orbit altitude and inclination and season also. Practical recommendations how to reduce the dispersion of ballistic reentry trajectory in the atmosphere and total heat flux are given on the basis of mathematical simulation.

Keywords: Ballistic Re-entry, Disturbed Atmosphere, Dispersion of Landing Point, Heating, Aerodynamics, Drag

Computational model of the Earth disturbed atmosphere

Computational Model of the Earth Disturbed Atmosphere - CMEDA was developed at the Keldysh Institute of Applied Mathematics (KIAM, Moscow) in 1968-1998 [1-2] .

The CMEDA is intended for

- development of vehicle guidance algorithms,
- estimation of expected accuracy of manoeuvre,
- determination of aerodynamic loads, etc.

The CMEDA is a global model for altitudes from 0 km up to 100 km and includes all 12 months of the year. It contains season-latitude, diurnal and random components of density variations and a wind field also. It allows to generate unlimited number of disturbed atmosphere samples for simulation of various flight conditions.

A variation of density $\delta\rho$ is represented as normalized deviation of disturbed density ρ from standard one ρ_{st}:

$$\delta\rho = (\rho - \rho_{st}) / \rho_{st} . \qquad (1)$$

The total variation includes season-latitude, diurnal and random components

$$\delta\rho = \delta\rho_{sl} (H,\varphi , N) + \delta\rho_{d} (H,\varphi , t) + \delta\rho_{r} (H, \lambda, \varphi, N, \bar{\xi}) \qquad (2)$$

where H is an altitude, φ is a latitude, λ is a longitude, N is a month number, t is a local time, $\bar{\xi}$ is a random vector.

The Reference Atmosphere CIRA 1986[3] with necessary updating is used for season-latitude variation of atmosphere density.

The model of amplitude and phase for diurnal component is constructed on the basis of the Reference Atmosphere CIRA 1972[4] and is identical for all months of a year.

Season-latitude and diurnal variations are systematic and describe a mean or expected state of atmosphere as function of altitude, latitude, month and local time. The random component determines a difference between "actual" state of atmosphere and systematic components. Limited experimental data and irregular allocation of measurement points complicate creation of an exact model of disturbed atmosphere. Thus, some reasonable hypothesis that does not contradict with observed processes in atmosphere is necessary to use. For example, the so called Model 4D (USA) uses Markov process for description of random density variations. The canonical-series expansion model was used for the re-entry simulation of the vehicle "Buran".

The method of normalizing functions was developed for the CMEDA. It is based on the analysis of experimental measurement data. Three normalizing functions $f_1(H, \bar{\xi})$, $f_2(\varphi, \bar{\xi})$ and $f_3(\lambda, \bar{\xi})$ allow to simulate the harmonic density variations as function of altitude, latitude and longitude. Developed model of limit variations ($3\sigma_\rho$) is used for this purpose also.

The model of wind contains zonal (along the parallel) and meridional components of a wind velocity. The zonal component U consists of three terms, season-latitude, diurnal and random:

$$U = U_{sl} + U_d + U_r . \qquad (3)$$

The meridional component has a random nature:

$$V = V_r . \qquad (4)$$

The Reference Atmosphere CIRA 1986[3] was used to build the season-latitude wind field model. The model of the diurnal and the random components of a wind is constructed utilizing geostrophic approximation.

CMEDA was used for investigation of landing point dispersion at ballistic re-entry in the Earth atmosphere.

Investigation of landing point dispersion

At ballistic re-entry in disturbed atmosphere a dispersion of landing point depends on

- initial parameters of motion (re-entry angle θ_{en} and velocity V_{en}, inclination of initial orbit i, latitude φ_0 and longitude λ_0 of re-entry point),
- ballistic coefficient of re-entry vehicle $\sigma_D = C_D S/m$,
- season (month).

Here C_D is a drag coefficient, S is a middle area, m is the vehicle mass.

Most important are initial parameters of motion and ballistic coefficient of re-entry vehicle. Consideration of season atmospheric variation is a new factor that allows to have a more accurate estimation of landing point dispersion.

For comparative analysis we fix a set of initial re-entry conditions (the basic point). Then we shall consider step-by-step a variation of each parameter to estimate its influence on landing accuracy and parameters of motion. We accept following conditions as the basic point:

- re-entry angle $\theta_{en0} = -3^o$, velocity $V_{en0} = 7722$ m/s,
- ballistic coefficient $\sigma_{D0} = 10^{-3}$ m^2/kg,
- month - January.

A longitude of re-entry point influence on landing accuracy is unessential, so we not consider its variation. The altitude of conditional boundary of atmosphere is H_{at}=100 km. The altitude of terminal point is H_t=10 km. The drag parachute system starts to operate approximately at this altitude. So, we consider a dispersion of landing point at altitude of 10 km. The basic values of re-entry angle and velocity correspond to de-boost by impulse of $\Delta V = 235$ m/s at initial circular orbit with altitude of $H_{cir} = 300$ km. The basic value of ballistic coefficient is approximately the same as for re-entry vehicles "Vostok", Mercury, "Soyuz" and Apollo. Variations of density and wind in January are extreme, so a dispersion of landing point is maximal also. For each set of initial conditions it is enough to calculate 100 re-entry trajectories in disturbed atmosphere. As a result we can determine a relative mean square dispersion of landing point $\tilde{\sigma}_x = \sigma_x / \sigma_{x0}$, a relative maximal load factor $\tilde{n}_{max} = n_{max}/n_{max0}$ and a relative descent time $\tilde{t} = t/t_o$. Index "0" corresponds to the basic point. Representation of results in dimensionless form allows to reduce the influence on conclusions of terminal point choice at altitude of 10 km. It is also convenient for comparative analysis. A cross range dispersion σ_Z is 5 ... 8 times less than σ_X and we can neglect it.

Fig. 1 illustrates the results of re-entry angle variation for initial equatorial orbit ($i = 0$, $\varphi_0 = 0$). A landing point is in equatorial zone. When the value of re-entry angle decreases from $|\theta_{en}| = 3^o$ to 2^o the relative descent time $\tilde{t}$ increases 1.25 times. The relative downrange dispersion $\tilde{\sigma}_x$ increases 1.7 times almost. The relative maximal load factor decreases to $\tilde{n}_{max}$ = 0.85. When the value of re-entry angle increases to 5^o the descent time decreases to 0.7 approximately and downrange dispersion decreases to 0.5 approximately. The maximal load factor increases ~ 1.4 times. Re-entry velocity variation in the range ± 300 m/s ($\pm 4\% V_{en0}$) produces variation of $\tilde{\sigma}_x$ within ± 0.3 and variation of $\tilde{n}_{max}$ within ± 0.08. Clearly that variation of re-entry velocity produces only a small change of re- entry trajectory. When the ballistic

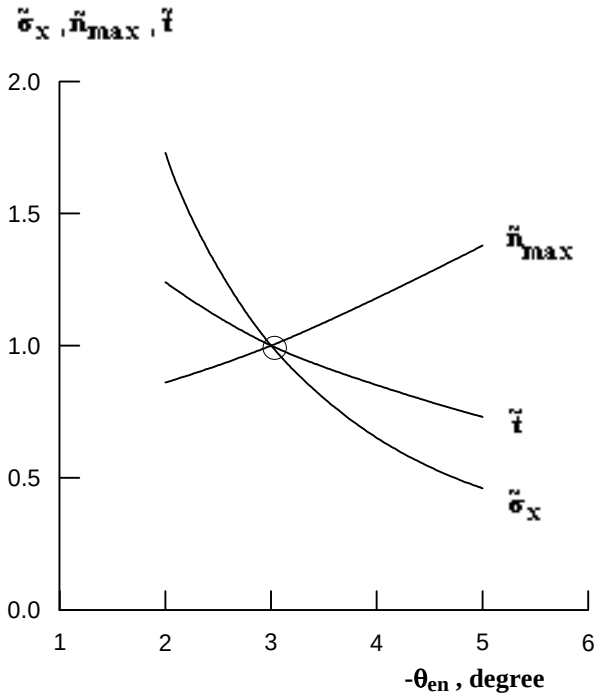

Figure. 1: Variation of re-entry angle (equatorial orbit i = 0)

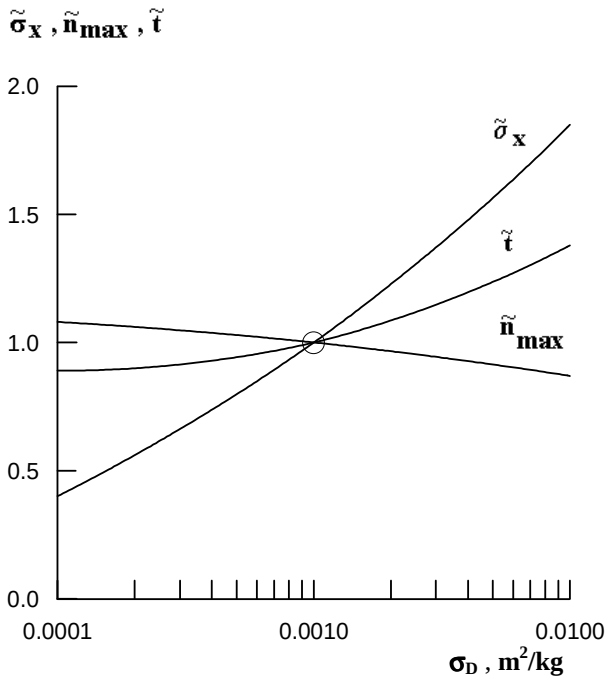

Figure 2: Variation of ballistic coefficient (equatorial orbit i = 0)

coefficient increases 10 times (i.e. $\sigma_D = 10^{-2}$ m^2/kg) the descent time increases ~ 1.4 times and downrange dispersion increases approximately 1.9 times (see Fig.2). If the ballistic coefficient decreases 10 times (i.e. $\sigma_D = 10^{-4}$ m^2/kg) the descent time decreases to $\tilde{t}$ = 0.9 and downrange dispersion decreases to $\tilde{\sigma}_x$ = 0.4. The maximal load factor $\tilde{n}_{max}$ does not depend on ballistic coefficient almost (it changes within ±0.1 only).

The season variation of atmosphere produces a small effect on downrange dispersion $\tilde{\sigma}_x$ at ballistic re-entry in the equatorial zone (see Fig. 3). The minimal dispersion (in October and April) differs from the maximal one (in January and July) by 0.1 only. Periodicity in 6 months is typical for re-entry in equatorial zone. It reflects the fact of quasi-symmetry of atmosphere in the northern hemisphere and southern one with shift on 6 months. The season variation does not influence on descent time $\tilde{t}$ and maximal load factor $\tilde{n}_{max}$ almost.

The initial orbit with inclination i = 40^o and latitude of re-entry point $\varphi_0 = 40^o$ corresponds to landing at mean latitudes of the northern hemisphere While re-entry angle θ_{en} variation the downrange

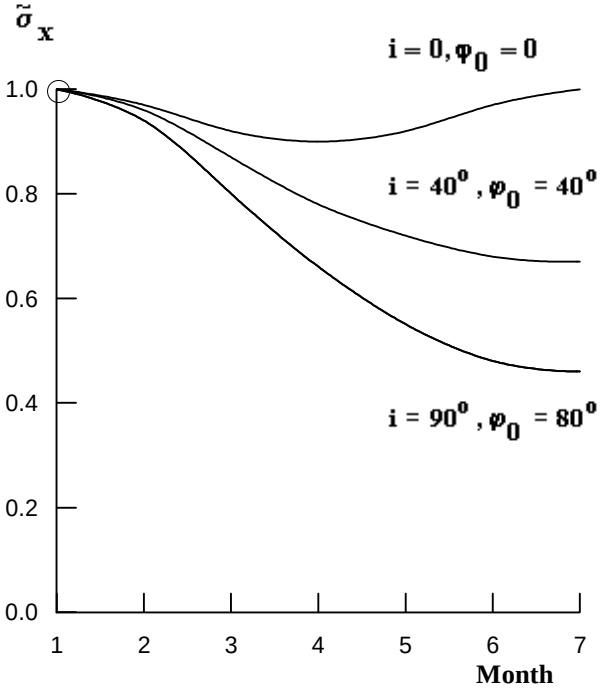

Figure 3: Season variation of dispersion

dispersion $\tilde{\sigma}_x$, the maximal load factor $\tilde{n}_{max}$ and descent time $\tilde{t}$ change as in equatorial zone approximately. Dimension values differ significantly. When re-entry velocity decreases by 300 m/s the downrange dispersion $\tilde{\sigma}_x$ decreases to 0.7. When re-entry velocity increases by 300 m/s the downrange dispersion $\tilde{\sigma}_x$ increases to 1.35. The maximal load factor $\tilde{n}_{max}$ and descent time $\tilde{t}$ change within ±0.1 (Fig. 4). If ballistic coefficient changes in wide range the downrange dispersion $\tilde{\sigma}_x$ and descent time $\tilde{t}$ have approximately the same change as in equatorial

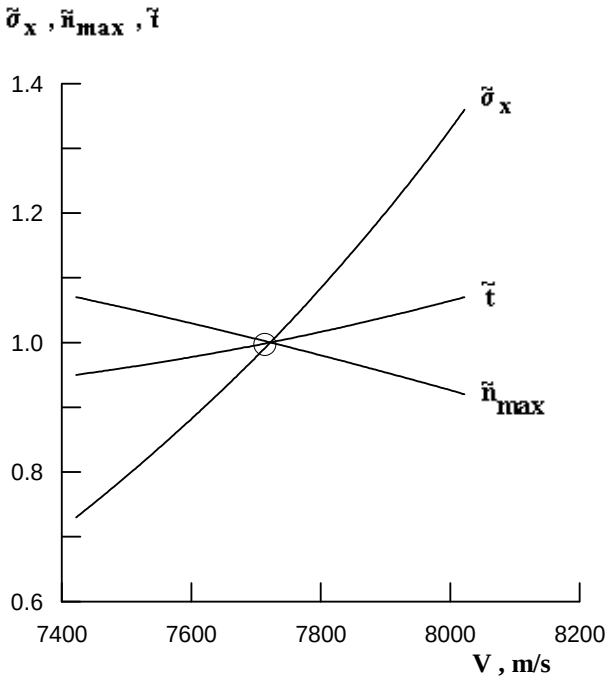

Figure 4: Variation of re-entry velocity (inclination i = 40°, φ0 = 40°)

zone, but dimension values differ significantly. Influence of season is more than for landing in equatorial zone (Fig. 3). The minimal dispersion is in summer: $\tilde{\sigma}_x$ = 0.7 due to minimal season-latitude density variation at altitudes of 30...70 km.

We considered landing in polar zone also to have the complete investigation (polar orbit i = 90°, latitude of re-entry point φ_0 = 80°). For re-entry angle variation the downrange dispersion $\tilde{\sigma}_x$, maximal load factor $\tilde{n}_{max}$ and descent time $\tilde{t}$ change as in equatorial zone and mean latitude almost. Dimension values have a big difference. The downrange dispersion $\tilde{\sigma}_x$ is more sensitive to re-entry velocity variation than at mean latitude (Fig. 5).

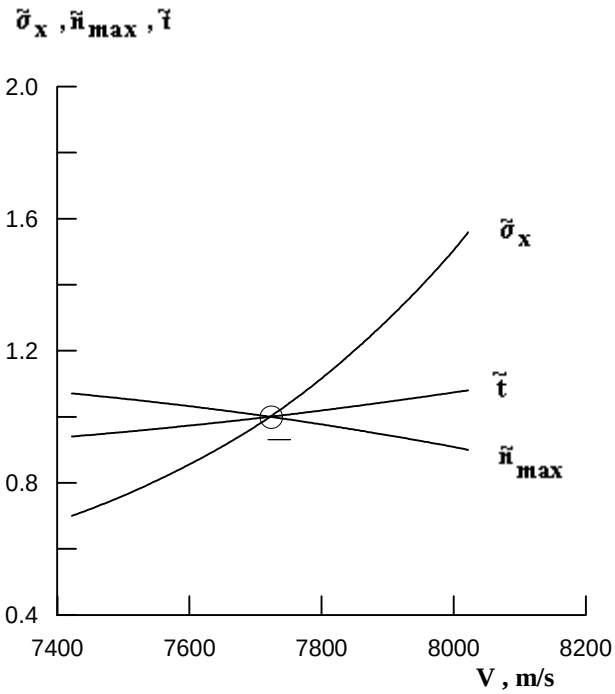

Fig. 5: Variation of re-entry velocity (inclination i = 90°, φ0 = 80°)

Variation of ballistic coefficient σ_D influences on $\tilde{\sigma}_x$, $\tilde{n}_{max}$ and $\tilde{t}$ as at equatorial zone and mean latitude almost. Effect of season is more significant (Fig. 3).

Fig. 6 illustrates influence of re-entry point latitude φ_0 on downrange dispersion $\tilde{\sigma}_x$ and maximal load factor $\tilde{n}_{max}$. Now the basic point is equatorial orbit (i = 0, φ_0 = 0). One can see that downrange dispersion and load factor increase as parabola approximately when latitude increases.

Choice of rational orbit and re-entry conditions

We use obtained results of landing point dispersion analysis and optimal re-entry manoeuvre consideration for preliminary design of SARA[5] mission scheme. SARA (SAtélite de Reentrada Atmosférica) is a Brazilian project of a small reusable ballistic re-entry vehicle. The vehicle is intended for delivery to the Earth of scientific results. Requirements to reusable re-entry vehicle do not agree with requirements to ballistic

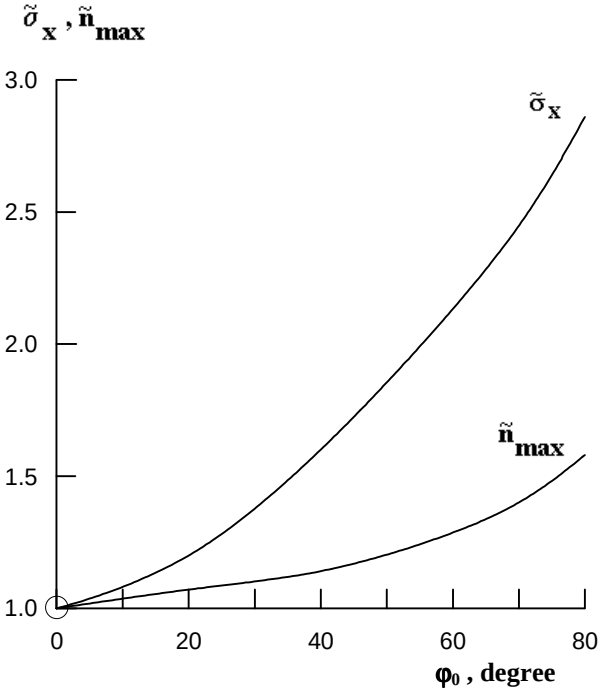

Figure 6: Variation of re-entry point latitude

descent trajectory and restricted dispersion of landing point. So, the solution should be a compromise.

Preliminary let us determine the *optimal radius of initial circular orbit* that provides the required re-entry angle θ^*_{en} by minimal value of de-boost impulse ΔV. A small de-boost impulse ΔV is directed against to orbital velocity V_{cir} (this direction is optimal[6]). In assumption of impulse velocity correction we can determine the minimal value of de-boost impulse $\Delta\tilde{V} = \Delta V/V_{cir}$ for given re-entry angle θ^*_{en} and fixed radius of circular orbit $\tilde{r}_{at} = r_{cir}/r_{at}$[6]:

$$\Delta\tilde{V} = 1 - \sqrt{\frac{2(\tilde{r}_{at} - 1)}{(\tilde{r}_{at}\sec\theta^*_{en})^2 - 1}}\,. \qquad (5)$$

From the necessary condition of optimality $d\Delta\tilde{V}/d\tilde{r}_{at} = 0$ we can determine the radius of the circular orbit

$$\tilde{r}_{opt} = (\tilde{r}_{at})_{opt} = 1 - \sin\theta^*_{en} \qquad (6)$$

that satisfies also the sufficient condition of optimality

$$\left.\frac{d^2\Delta\tilde{V}}{d\tilde{r}_{at}^{\,2}}\right|_{\tilde{r}_{opt}} > 0\,. \qquad (7)$$

The minimal value of de-boost impulse at optimal orbit is

$$\Delta\tilde{V}_{min} = 1 - \cos\frac{\theta^*_{en}}{2} - \sin\frac{\theta^*_{en}}{2}\,. \qquad (8)$$

Fig. 7 shows an altitude of optimal circular orbit H_{opt} and minimal required de-boost impulse ΔV_{min} for the given value of re-entry angle θ^*_{en}. Obtained recommendations we can use in practice only for small re-entry angles $|\theta^*_{en}| \le 3^0$. Really, for the given angle in the range $|\theta^*_{en}| = 1^0...3^0$ the altitude of optimal circular orbit is 200 km ... 438 km. A payload capability of launch vehicle decreases very sharply with increase of orbit altitude above 200 ... 250 km. Thus the economy of de-boost impulse (and propellant consumption m_{pr} accordingly) can not compensate payload loss due to increase of orbit altitude.

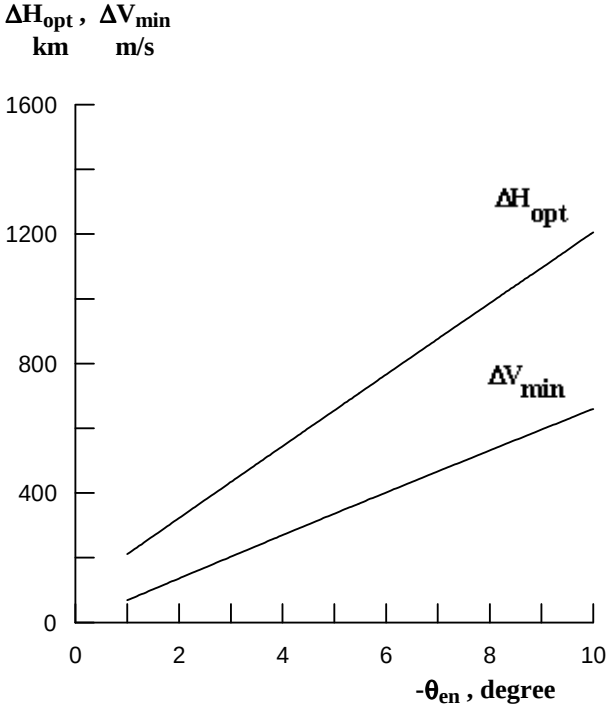

Fig. 7: Altitude of optimal circular orbit and minimal required impulse

The optimal orbit satisfies the ballistic aspect of re-entry task only and is of theoretical interest more than practical one. So, it is necessary to consider the *rational orbit* that takes into account payload capability of the launch vehicle also. Therefore the rational orbit represents a compromise between decrease of payload and decrease of required propellant consumption with increase of orbit altitude.

As an example we consider the Brazilian launch vehicle VLS[7] and re-entry vehicle SARA[8] type (initial mass m_0 = 150 kg). All calculation results are represented as variations with respect to basic point (circular orbit with altitude of H_{cir} = 300 km, de-boost impulse ΔV = 235 m/s, re-entry angle θ_{en}^{*} = -3^0). For such value of re-entry angle the optimal orbit has an altitude of H_{opt} = 438 km and the minimal required de-boost impulse is ΔV_{min} = 203 m/s. Clearly that rational orbit should be below H_{opt}. With equation (5) we can calculate a value of required de-boost impulse ΔV for given re-entry angle θ_{en}^{*} =-3^0 as function of orbit altitude H_{cir} (Fig. 8). Then the equation for characteristic velocity allows us to estimate a propellant consumption for realization of required impulse ΔV (velocity of jet efflux W = 2000 ... 3000 m/s).

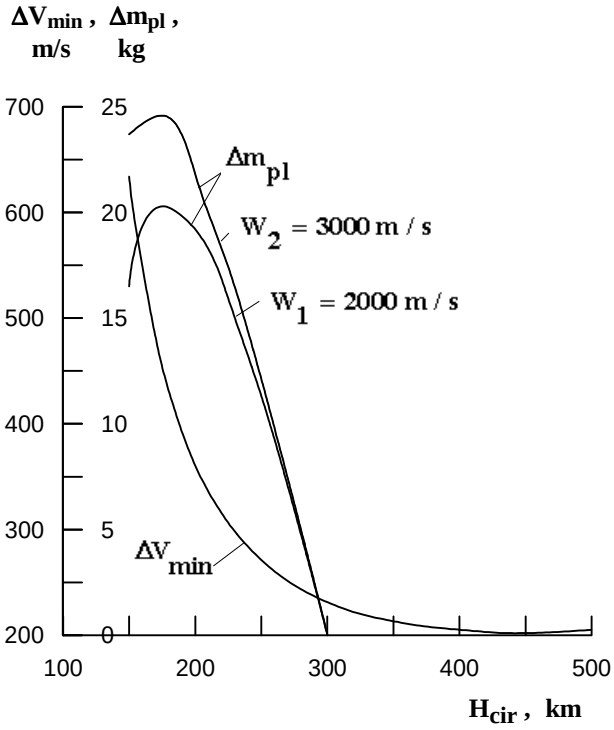

Fig. 8. Determination of rational orbit

For VLS derivative of payload mass with respect to altitude of orbit is

$$\frac{\partial m_{pl}}{\partial H_{cir}} = -0.28\frac{kg}{km}. \qquad (9)$$

Now we can estimate how the payload increases if the orbit altitude decreases with respect to basic point H_{cir} = 300 km. For the orbit H_{cir} = 250 km the payload increases by Δm_{pl} = 10 kg (~7% of SARA basic mass m_0 = 150 kg). For the orbit H_{cir} = 200 km the payload increases by Δm_{pl} = 20...24 kg (see Fig.8). So, we should choice the altitude of rational orbit in the range 200...300 km according to required life time of satellite.

Now let us estimate heat flux and its dependence on the ballistic coefficient and re-entry conditions. For the model task in assumptions of descent with constant flight path angle θ = constant in exponential atmosphere we can determine a heat flux [9]. The maximal heat flux per second in critical point is

$$(q_{cr})_{max} = k_{lam} V_{en}^{\,3} \sqrt{-\frac{\lambda \sin\theta_{en}}{3e\sigma_D}} \qquad (10)$$

and the total amount of heat received by vehicle during descent into the atmosphere is

$$Q = \frac{1}{4\sigma_D} C_{fr} S_{\Sigma} V_{en}^{\,2} \left[1 - exp\left(-\frac{\sigma_D \rho_0}{\lambda \sin|\theta_{en}|} \right) \right]. \qquad (11)$$

Here k_{lam} is a coefficient of laminar boundary layer, λ is a logarithmic gradient of density, e = 2.718..., C_{fr} is an equivalent coefficient of surface friction, S_{Σ} is a total area of vehicle surface, ρ_0 is the model density at the Earth surface.

The value of $(q_{cr})_{max}$ decreases when ballistic coefficient σ_D increases and re-entry angle $|\theta_{en}|$ decreases. The total amount of heat Q received by vehicle during descent into the atmosphere decreases when the ballistic coefficient σ_D increases and re-entry angle $|\theta_{en}|$ increases also. Therefore it is necessary to provide as bigger as possible ballistic coefficient σ_D. It means that aerodynamic shape of re-entry vehicle should be "bad" with a big radius of the nose part curve.

As mentioned above, when SARA type vehicle de-boosts at circular orbit H_{cir} = 300 km by impulse ΔV = 235 m/s it has re-entry angle θ^*_{en} = -3^0 and re-entry velocity V_{en} = 7722 m/s. We can consider as a basic point the descent into atmosphere by sharp side forward (ballistic coefficient is σ_D = 0.00213 m^2/kg , relative downrange dispersion $\tilde{\sigma}_x$ = 1 , relative maximal load factor $\tilde{n}_{max}$ = 1). All results are obtained by statistic simulation of re-entry trajectories in disturbed atmosphere (model CMEDA).

When re-entry vehicle moves by wide side forward (ballistic coefficient is σ_D = 0.0064 m^2/kg) the downrange dispersion is $\tilde{\sigma}_x$ = 1.35 and maximal load factor is $\tilde{n}_{max}$ = 0.9. Now heating conditions should be better due to 3 times bigger value of ballistic coefficient.

If it is necessary to provide the same downrange dispersion as in basic point we should increase the value of re-entry angle to $|\theta^*_{en}|$ = 4^0 (de-boost impulse ΔV = 360 m/s, re-entry velocity V_{en} = 7600 m/s). In the case downrange dispersion is $\tilde{\sigma}_x$ = 0.9, the maximal load factor $\tilde{n}_{max}$ = 1.1 but another heating condition. Such comparison with the basic point is more correct because downrange dispersion is the same approximately.

Aerodynamic heating due to high velocity

At ballistic re-entry high heat flux rates and high surface temperatures will be a severe requirement for development of the thermal protection system.

With the aim to reduce the heat flux rate and consequently the surface temperature a parametric study has been done considering variation of re-entry angle θ_{en} and drag coefficient C_D. For the re-entry angle θ_{en} two values were assumed: a) - 3° with re-entry velocity Ven = 7722 m/s, and b) - 4° with re-entry velocity Ven = 7600 m/s. The drag coefficient was estimated for different vehicle shapes as shown below.

Calculating now the heating rates and maximal temperatures during re-entry in the Earth atmosphere, the results shown in the following table are obtained[10].

The calculation model assumes a non-ablative re-radiating surface (ceramic material). The results presented in the above table are maximal values which correspond to stagnation conditions.

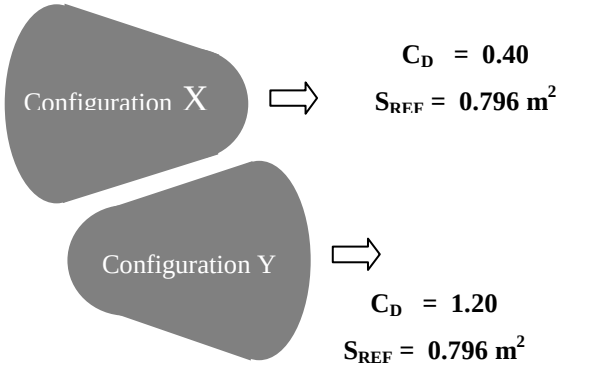

Case	Drag Coeff.	Re-entry angle	Heat flux [kW/m^2]	Temperature [K]
X1	0.40	-3º	2550	2640
Y1	1.20	-3º	700	1880
Y2		-4º	810	1990

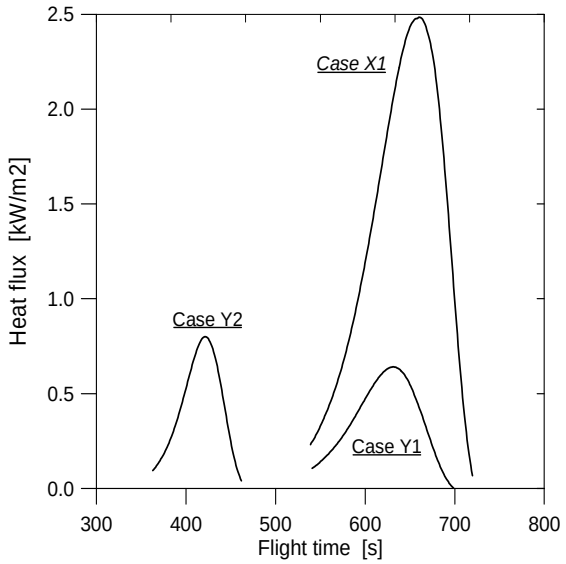

Fig. 9. Heat flux as function of flight time

With increasing drag coefficient, configuration Y, the heat flux and consequently the maximal temperature decays substantially due to firstly reduction of the velocity at high altitudes and of major importance the much higher nose radius. Increasing the re-entry angle for the configuration Y the heat flux and the temperature increases slightly due to a higher re-entry velocity for θ_{en} = - 4°.

With these results a first attempt should be made considering that lower heat flux and lower temperature

levels will make possible the use of conventional materials for the thermal protection systems.

Landing point dispersion analysis required calculation of approximately 5,000 trajectories in disturbed atmosphere (model CMEDA).

Conclusions

Investigation of landing point dispersion for descent in disturbed atmosphere (model CMEDA) allows to make conclusions as following.

1. Re-entry angle θ_{en} and latitude φ_0 of re-entry point are the most important initial parameters those determine downrange dispersion σ_x and maximal load factor n_{max}.

2. When the ballistic coefficient σ_D increases 10 times the downrange dispersion increases 2 times approximately. When the ballistic coefficient σ_D decreases 10 times the downrange dispersion decreases two times approximately. The maximal load factor n_{max} does not depend on the ballistic coefficient practically.

3. By choice of month (if it is possible) we can decrease the downrange dispersion σ_x on 10% for landing in equatorial zone, on ~30% for landing in mean latitude and on 50% for landing in polar zone.

4. Increasing three times the drag coefficient and keeping the re-entry angle equal to -3º minimal heat flux and temperature at the stagnation point are reached.

Obtained recommendations allow to choice (in admissible situations) the optimal re-entry conditions and reduce the downrange dispersion σ_x or/and maximal load n_{max}.

References

[1] Sikharulidze, Y G.; Kaluzhskikh, Y. N.; Kostochko, P. M. Computational Model of the Earth Disturbed Atmosphere and a High Accuracy Re-entry Guidance for a Vehicle with Average Lift-to-Drag Ratio. *Proceedings of the 12-th International Symposium on Space Flight Dynamics*, Darmstadt, Germany, 1997.

[2] Korchagin, A. N.; Kostochko, P. M.; Sikharulidze, Y. G. Computational Model of the Earth Disturbed Atmosphere. *Space Research Journal*, 1998 (to be published).

[3] CIRA 1986 (COSPAR International Reference Atmosphere 1986). *Adv. in Space Res.* Vol.8, No. 5-6, 1988.

[4] CIRA 1972 (COSPAR International Reference Atmosphere 1972). 1972, Berlin.

[5] Moraes, P. Jr., Pilchowski, H.-U. Plataforma Orbital Recuperável para Experimentação em Ambiente de Microgravidade. *XIV Brazilian Congress of Mechanical Engineering*, Bauru-SP, 1997.

[6] Sikharulidze, Y.G. Optimal De-orbit for Re-entry. *Space Research Journal*, Vol.8, No.2, 1970.

[7] Boscov, J. et alli. Development Status of the Brazilian VLS Satellite Launcher Program, *17th International Symposium on Space Technology and Science*, Tóquio, Japão, Mai 90

[8] Moraes, P. Jr. Design Aspects of the Recoverable Orbital Platform SARA. *8º Congreso Chileno de Ingenieria Mecánica*, Concepción, Chile, 1998.

[9] Yaroshevsky, V.A. Spacecraft Re-entry in the Atmosphere. Moscow, "Nauka", 1988 (book in Russian).

[10] Pessoa Filho, J. B., Moraes, P. Jr. Redução do Fluxo Térmico e da Temperatura no Veículo SARA através da Modificação da sua Forma. *CTA/IAE, NT-154/ASE-N/98 (internal report)*, 1998.